

Magnetic flux dynamics and structural features in fluorinated $\text{HgBa}_2\text{CuO}_4$ as probed by ^{19}F NMR

A. A. Gippius* and E. N. Morozova

Department of Physics, Moscow State University, 119899 Moscow, Russia

E. V. Antipov, A. M. Abakumov, and M. G. Rozova

Department of Chemistry, Moscow State University, 119899 Moscow, Russia

K. Lüders and W. Hoffmann

Department of Physics, Free University of Berlin, D-14195 Berlin, Germany

G. Buntkowsky and O. Klein

Department of Chemistry, Free University of Berlin, D-14195 Berlin, Germany

(Received 27 October 1999)

^{19}F NMR spectra and spin-lattice relaxation rates have been measured on two powder $\text{HgBa}_2\text{CuO}_4\text{F}_x$ samples. The results combined with our neutron powder-diffraction data [A. M. Abakumov *et al.*, Phys. Rev. Lett. **80**, 385 (1998)] confirm that fluorine atoms can be successfully incorporated in the lattice of superconducting Hg-1201 phase in the nonstoichiometric O3 site. Partial occupation of another oxygen position by fluorine atoms reveals to be possible with the increase of F content. The temperature dependence of the ^{19}F NMR linewidth reveals the crossover at 35 K in the magnetic-flux line structure between the low-temperature latticelike regime and high-temperature “melted” regime. For the $1/T_1$ temperature dependence a maximum has been found at 65 K indicating the strong influence of magnetic-flux line motion on the ^{19}F spin-lattice relaxation rate.

The T_c values of $\text{HgBa}_2\text{CuO}_{4+\delta}$ (Hg-1201) superconductors can be easily varied over a wide range (from strongly underdoped to optimally doped or even a highly overdoped nonsuperconducting state) by insertion of O^{2+} or F^- anions in the Hg layer. The maximum T_c values for oxygenated and fluorinated Hg-1201 are exactly the same (97 K), while the amount of inserted fluorine ($\delta_F=0.24$) is twice that of oxygen ($\delta_O=0.12$) and this supports a simple ionic doping model.¹ This cation replacement does not affect significantly the Hg-1201 structure and therefore ^{19}F nuclei provide an excellent microscopic NMR probe of the magnetic-flux line (FL) behavior as well as structural peculiarities of the fluorinated Hg-1201 superconductors due to their high NMR sensitivity and the absence of an electric quadrupole moment. We present here an unambiguous evidence from ^{19}F NMR that fluorine atoms are successfully incorporated in the superconducting matrix of Hg-1201. Our results evidently show the efficiency of ^{19}F NMR probe to investigate the phase diagram of the vortex state in high- T_c superconductors.

Single-phase samples of $\text{HgBa}_2\text{CuO}_{4+\delta}$ were synthesized from a mixture of $\text{Ba}_2\text{CuO}_{3+\delta}$ and HgO according to the procedure described in Ref. 2, then reduced in dynamic vacuum to the composition $\text{HgBa}_2\text{CuO}_{4.01}$ ($T_c=61$ K) determined by iodometric titration. Fluorination of the reduced Hg-1201 sample was carried out using XeF_2 as the fluorinating agent. Details of the synthesis are described in Ref. 1. For our measurements we used two powder $\text{HgBa}_2\text{CuO}_4\text{F}_x$ samples (hereafter sample 1F and sample 2F) prepared under different conditions: with 0.1 XeF_2 at 150 °C for the sample

1F and with 0.3 XeF_2 at 200 °C for the sample 2F. Sample 2F has been prepared under stronger fluorination conditions and exhibits a slightly reduced $T_c=96$ K and smaller lattice parameters [$a=3.8825(3)$ Å, $c=9.510(1)$ Å] in comparison with those for the sample 1F [$T_c=97$ K, $a=3.8828(4)$ Å, $c=9.523(1)$ Å]. Thus we can assume that the fluorine content in the sample 2F is higher than in the sample 1F although we have no direct measure of the fluorine content in these samples. All samples were single phase compounds as characterized by x-ray powder-diffraction technique; sample 2F was characterized also by neutron powder diffraction (NPD).¹

The T_c values were determined by ac magnetization measurements.¹ The ^{19}F NMR experiments were performed at magnetic field of 7.01 T in the temperature range of 4.2–300 K. The ^{19}F NMR spectra were obtained by the Fourier transform of the echo signal after $(\pi/2-\pi)$ pulse sequence using simple four-phase cycling technique. The fluorine nuclear spin-lattice relaxation rate was measured using the saturation recovery method.

Typical ^{19}F NMR spectra of the sample 1F measured at different temperatures are presented in Fig. 1. As reference frequency F_0 we use the resonance frequency of the bare ^{19}F nuclei with the gyromagnetic ratio $^{19}\gamma=40.0538$ MHz/T.³ No measurable shift has been found with respect to the reference frequency F_0 . Similar absence of the ^{19}F shift has been reported by Wani *et al.*⁴ for fluorinated $\text{YBa}_2\text{Cu}_4\text{O}_8$ and reflects the quasi-two-dimensional (2D) character of superconductivity in the layered cuprates with an extremely low density of charge carriers outside the CuO_2 layers. The spec-

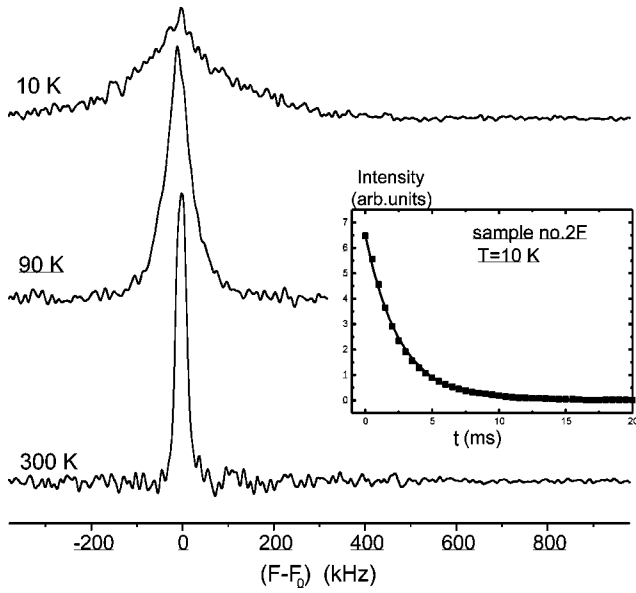


FIG. 1. ^{19}F NMR spectra of the sample 1F measured at different temperatures. Inset: example of the fitting of the half echo intensity decay by Eq. (1) in the sample 2F (see text).

tra of both $\text{HgBa}_2\text{CuO}_4\text{F}_x$ compounds exhibit a single line without additional peaks and shoulders which yields the additional proof that our samples contain only the single fluorinated phase. The spectral linewidths $\Delta\nu$ at half maximum vs temperature are plotted in Fig. 2. Both samples show nearly the same $\Delta\nu(T)$ dependence in the whole temperature range 10–300 K. Above T_c the linewidth is almost temperature independent: $\Delta\nu \approx 30$ kHz at 100 K and $\Delta\nu \approx 20$ kHz at 300 K which is close to the values recently obtained by Goren *et al.*⁵ in a series of $\text{YBa}_2\text{Cu}_3\text{O}_x\text{F}_y$ compounds. Below T_c the spectra exhibit rapid broadening with decreasing temperature. Such a behavior is characteristic for NMR spectra in the mixed phase of type-II superconductors where the line broadening below T_c is caused by an inhomogeneous distribution of the magnetic field in the flux-line lattice. This result is clear and direct evidence that fluorine atoms are successfully incorporated in the superconducting matrix of Hg-1201. The NPD data gave us only indirect support showing

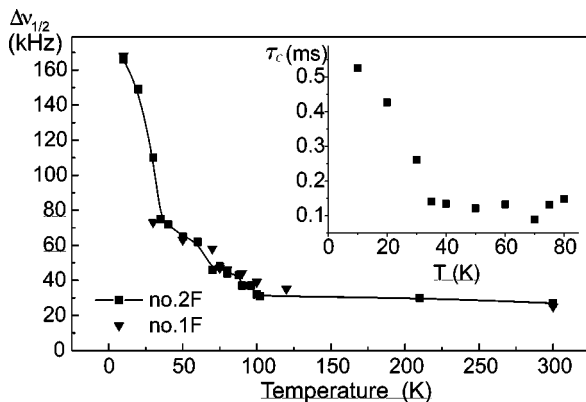


FIG. 2. Temperature dependences of ^{19}F NMR linewidths for the samples $\text{HgBa}_2\text{CuO}_4\text{F}_x$. Inset: correlation time τ_c of magnetic FL motion extracted from half echo decay by fitting to Eq. (1) in the time domain (see text).

twice amount of anion in the O3 site in comparison with an oxygenated sample with the same T_c ,¹ but NPD could not distinguish O and F due to their close scattering lengths. However, combined with the NMR result it reveals that F is inserted in the O3 position which was almost empty in the initial reduced Hg-1201 phase and has the occupation number 0.24 in the sample 2F.¹

The remarkable feature of the observed ^{19}F linewidth temperature dependence is the existence of the well pronounced crossover for both samples at about $T_{cr} \approx 35$ K. The similar crossover has been observed for ^{89}Y and ^{19}F in $\text{YBa}_2\text{Cu}_4\text{O}_8:\text{F}$,⁶ ^{89}Y in $\text{YBa}_2\text{Cu}_4\text{O}_8$,^{7,8} ^{89}Y in $\text{YBa}_2\text{Cu}_3\text{O}_{7-\delta}$,⁹ and ^{19}F in $\text{YBa}_2\text{Cu}_3\text{O}_{6.7}\text{F}_{0.2}$,²⁴ and was attributed to flux line (FL) motion. Following the simplified approach developed there (for detailed analysis see Ref. 25) the free induction decay (FID) in the presence of random Brownian motion is given by¹⁰

$$s(t) = \exp\{-\gamma^2 \langle \Delta B_{FL}^2 \rangle \tau_c^2 \cdot [\exp(-t/\tau_c) - 1 + t/\tau_c]\}. \quad (1)$$

Here τ_c is the characteristic correlation time of FL motion; $\langle \Delta B_{FL}^2 \rangle$ is the second moment of the magnetic-field distribution in the rigid FL lattice: $\langle \Delta B_{FL}^2(T) \rangle \sim [\Delta\nu^2(T) - \Delta\nu^2(300)]$. To extract the τ_c values the NMR spectra were fitted in Refs. 6–9 by the Fourier transform of the expression (1). In order to minimize the data manipulation errors we used Eq. (1) directly to fit the half echo intensity decay in the time domain (see the inset in Fig. 1) assuming the temperature dependence of $\Delta\nu_{FL}(T) = \Delta\nu_{FL}(0)[1 - (T/T_c)^4]$ as predicted by the London two-fluid model. The resulting τ_c values as a function of temperature are plotted in the inset of Fig. 2. Corresponding to the crossover on the linewidth the temperature dependence $\tau_c(T)$ also exhibits the clear crossover at $T_{cr} \approx 35$ K. It is well known that the B - T phase diagram of the superconducting state in the high- T_c cuprates is rather complicated due to the interplay of three energies which determine the state of the fluxoid lattice, namely the elastic energy of the fluxoid lattice (U_e), the pinning energy (U_p), and the thermal energy ($U_T = k_B T$).¹¹ At low temperatures where $U_T \ll (U_p, U_e)$ the fluxoids are considered to be in the latticelike state with the translational order over a certain range. The thermal energy U_T increases with T and reaches U_p at temperature T_{dp} where depinning of the latticelike fluxoids occurs. Finally, at temperatures above T_m , U_T exceeds $U_e + U_p$ and fluxoids are in the liquid state. For low- T_c superconductors with strong flux pinning such as Nb_3Sn , the depinning line $T_{dp}(H)$ is close to the melting line $T_m(H)$, while for high- T_c superconductors $T_{dp}(H)$ is below $T_m(H)$ and coincides with the irreversibility line $T_{irr}(H)$.^{11,12} Since the NMR linewidth depends on the second moment $\langle \Delta B_{FL}^2 \rangle$ of the magnetic-field distribution it is strongly affected by the melting of the FL lattice but not so much by its depinning. Therefore the observed crossover at $T = 35$ K on linewidth and correlation time temperature dependences is related to the melting temperature T_m . This temperature is, however, not far above T_{irr} for Hg-1201 which is about 28–30 K at the magnetic field of our experiment ($H = 7$ T).^{13,14}

The typical ^{19}F magnetization recovery curve after saturation sequence for the sample 1F with the lower fluorine

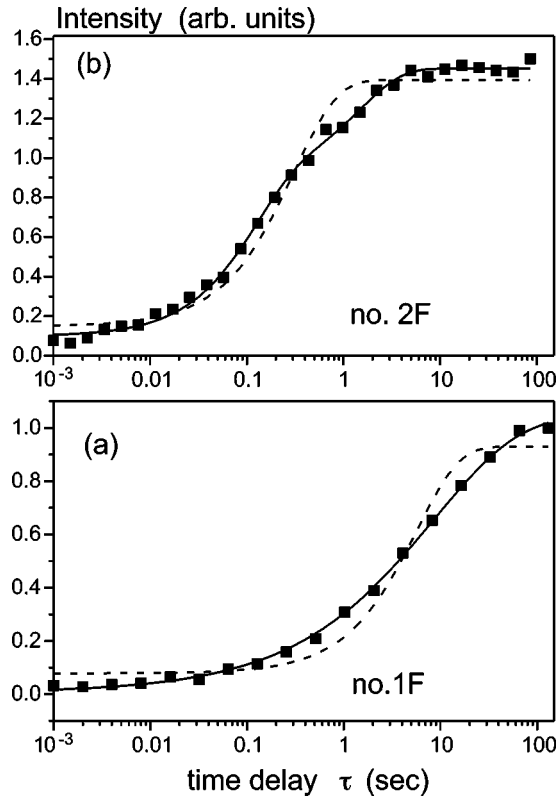


FIG. 3. ^{19}F magnetization recovery curve measured at 90 K for different $\text{HgBa}_2\text{CuO}_4\text{F}_x$ samples: (a) sample 1F: stretched exponential fit (solid line), single exponential fit (dashed line); (b) sample 2F: double exponential fit (solid line), single exponential fit (dashed line).

content is presented in Fig. 3(a). As seen from this figure, an attempt to fit the recovery curve by the single exponential function gives a systematic deviation from the experimental points. We found that for the sample 1F in the whole temperature range 10–300 K the echo intensity I is perfectly described by the stretched exponential dependence:

$$I = A - B \cdot \exp(-\tau/T_1)^n, \quad (2)$$

where T_1 is the spin-lattice relaxation time; τ is the time delay between the saturation sequence and the spin-echo sequence. The values of the parameter n were close to 0.5 varying in the narrow range of 0.45–0.57 for all temperature points. In order to avoid an additional degree of freedom in the T_1 determination we fixed the value $n=0.5$ in the fitting procedure. The stretched exponential function (2) with $n=0.5$ is a particular case of Kohlrausch's anomalous relaxation law $I \sim \exp[-(t/\tau)^\beta]$ ($0 < \beta < 1$) and is widely used in the description of relaxation processes in disordered systems like glasses (see Refs. 15 and 16, for instance). Recently, the stretched exponential recovery has been observed for the copper quadrupole relaxation in $\text{Sr}_{14}\text{Cu}_{24}\text{O}_{41}$ (Ref. 17) and in $\text{PrBa}_2\text{Cu}_3\text{O}_7$ (Ref. 18) indicating a spatial charge fluctuation in these materials. In general, the origin of the stretched exponential relaxation is the spatial distribution of relaxation rates of different nuclei which gives Eq. (2) after averaging over the space. For instance, this can be due to the dipolar interaction with a small amount of paramagnetic impurity atoms statistically distributed over the host lattice, which

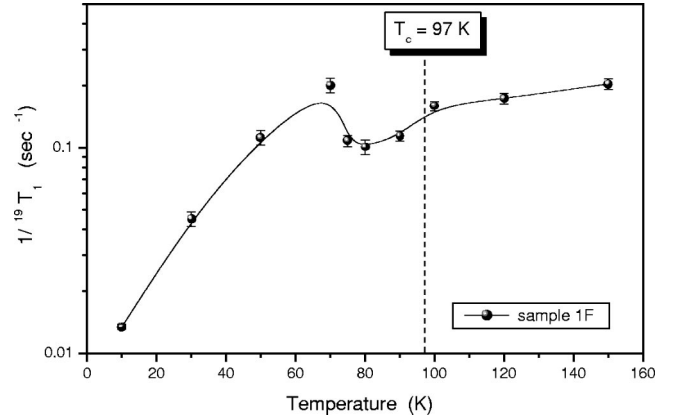


FIG. 4. Temperature dependence of ^{19}F NMR spin-lattice relaxation rates for $\text{HgBa}_2\text{CuO}_4\text{F}_x$ sample 1F. The solid line is just a guide for eye.

gives Eq. (2) with $n=0.5$.¹⁵ The relaxation via uncontrolled magnetic impurities can be ruled out since then one could expect the stretched exponential recovery also for ^{199}Hg nuclei which has not been observed in the experiment. The direct dipolar ^{19}F - ^{19}F interaction cannot be the reason as well because of low values of the nuclear dipolar magnetic fields. The possible mechanism might be the transferred hyperfine interaction¹⁹ of ^{19}F nuclei with Cu electronic spins via the path: ^{19}F -Hg-O2(apical)-Cu. This interaction is expected to be isotropic which coincides with the observed symmetric ^{19}F NMR line shape. Since the exchange interac-

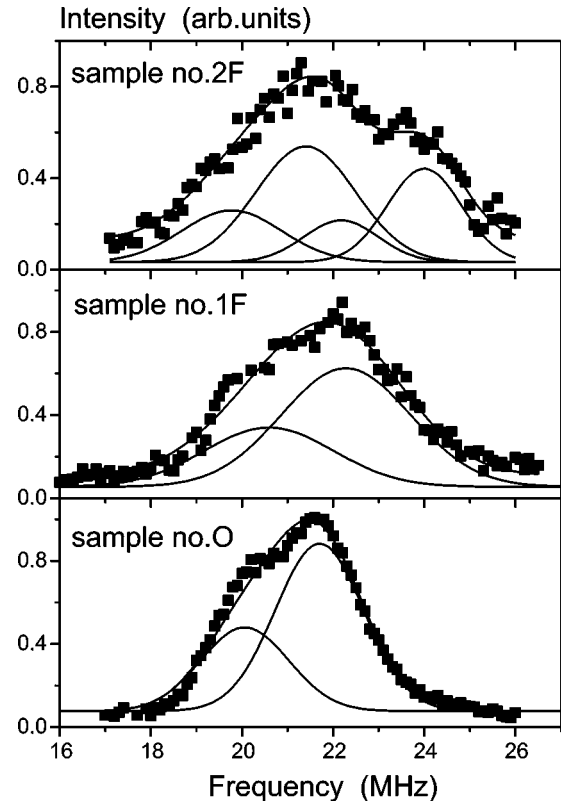


FIG. 5. Copper NQR spectra of $\text{HgBa}_2\text{CuO}_4\text{F}_x$ [samples 2F (upper), 1F (middle)], and $\text{HgBa}_2\text{CuO}_{4.13}$ (bottom) measured at 4.2 K. Gaussian fit for each Cu isotope and the resulting best fit are shown by solid lines.

tion path for each ^{19}F nucleus strongly depends on the occupation of the O3 positions in four neighboring Hg-Hg meshes the hyperfine interaction constant is statistically distributed over the O3 sites in the Hg-1201 matrix. This distribution is also reflected in the Lorentzian line shape of ^{19}F NMR spectra (see Fig. 1).

The resulting temperature dependence of the spin-lattice relaxation rate $R_1(T)$ for the sample 1F is shown in Fig. 4. The experimental ^{19}F spin-lattice relaxation rate exhibits several interesting features. First, the T_c influence on the spin-lattice relaxation is not so strong as for other nuclei in high- T_c superconductors. This coincides with the negligible Knight shift of the ^{19}F NMR line and can be attributed to the low density of charge carriers in the O3 position of the Hg layers. Second, the existence of the maximum at around $T_{\text{max}} \approx 65$ K has been observed on the $1/T_1$ temperature dependence for the sample 1F and on both $1/T_1$ components for the sample 2F. Earlier a similar behavior of the $R_1(T)$ dependence was observed in Y-124 and $\text{HgBa}_2\text{CuO}_{4+\delta}$ oriented powder samples for ^{89}Y , ^{19}F , and ^{199}Hg nuclei^{6,8,14} as well as for ^1H in organic superconductors²⁰ and was attributed there to the influence of the thermal fluctuations of the flux lines on the nuclear spin-lattice relaxation. It should be noted that in the vicinity of T_c this influence becomes less effective due to the process of transformation of the 2D pancake vortices to the conventional Abrikosov lines when the correlation length $\xi_c \sim 1/\sqrt{1 - T/T_c}$ exceeds the spacing between CuO_2 layers.²¹ This strongly reduces the fluctuating transverse magnetic field.

In contrast to the sample 1F, for the sample 2F with higher fluorine content the recovery of the nuclear magnetization exhibits a characteristic kink at time delay $\tau \approx 1$ sec [see Fig. 3(b)] and therefore is best described by a double

exponential function with one order of magnitude difference between the rates of fast and slow relaxation components for the sample 2F. This yields the evidence that at higher doping level a part of fluorine atoms occupies another oxygen position and exhibits a fast nuclear spin-lattice relaxation due to proximity to the copper site. This coincides with the observation of the second pair of copper lines in the NQR spectrum of the sample 2F whereas in the sample 1F we observed only one pair of Cu NQR lines (Fig. 5) which is similar to that for the optimally oxygen doped $\text{HgBa}_2\text{CuO}_{4.13}$ sample without fluorine (sample O) previously studied by NQR (Ref. 22) and NMR (Ref. 23) (sample 5 in Refs. 22 and 23) (Fig. 5). We can suppose that like an occupation of the O3 position the substitution of F for another O site occurs statistically without forming macroscopic regions in the lattice. This is confirmed by the absence of any kink on the ac-magnetization curve¹ which appears usually in the case of macroscopic phase mixture.

In conclusion, the application of ^{19}F NMR to fluorinated $\text{HgBa}_2\text{CuO}_{4+\delta}$ compounds confirms that fluorine atoms can be successfully incorporated in the lattice of superconducting Hg-1201 phase in the nonstoichiometric O3 site. Partial occupation of another oxygen position by fluorine atoms appears to be possible with the increase of F content. Sharp narrowing of ^{19}F NMR line above 35 K manifests melting of the fluxoid lattice.

The authors express their special gratitude to M. Mehring, C. Slichter, Y. Berthier, and A. Rigamonty for the interest to this work and for fruitful discussions during Specialized Colloque Ampere. We are also thankful to N. Brilliantov for important remarks. This work was supported by the ‘‘Volkswagen-Stiftung, Federal Republik of Germany,’’ Grant No. 1/73680.

*Author to whom correspondence should be addressed. FAX: 007-095-3625576. Electronic address: gippius@mail.ru

¹A. M. Abakumov *et al.*, Phys. Rev. Lett. **80**, 385 (1998).

²V. A. Alyoshin *et al.*, Physica C **255**, 173 (1995).

³*NMR Frequency Table*, Bruker Almanac (Bruker GmbH, Karlsruhe, 1999).

⁴B. N. Wani *et al.*, Physica C **272**, 187 (1996).

⁵S. D. Goren *et al.*, Physica C **304**, 283 (1998).

⁶M. Corti *et al.*, Physica C **291**, 297 (1997).

⁷Pietro Carretta, Phys. Rev. B **45**, 5760 (1992).

⁸M. Corti *et al.*, Phys. Rev. B **54**, 9469 (1996).

⁹P. Carretta and M. Corti, Phys. Rev. Lett. **68**, 1236 (1992).

¹⁰A. Abragam, *The Principles of Nuclear Magnetism* (Clarendon, Oxford, 1961), p. 439.

¹¹T. Matsushita, Physica C **214**, 100 (1993).

¹²K. Watanabe, Jpn. J. Appl. Phys., Part 2 **31**, L1586 (1992).

¹³U. Welp *et al.*, Physica C **218**, 373 (1993).

¹⁴B. J. Suh *et al.*, Phys. Rev. Lett. **76**, 1928 (1996).

¹⁵D. Tse and S. R. Hartmann, Phys. Rev. Lett. **21**, 511 (1968).

¹⁶R. G. Palmer *et al.*, Phys. Rev. Lett. **53**, 958 (1984).

¹⁷M. Takigawa *et al.*, Phys. Rev. B **57**, 1124 (1998).

¹⁸B. Grevin *et al.*, Phys. Rev. Lett. **80**, 2405 (1998).

¹⁹M. Mehring, Appl. Magn. Reson. **3**, 383 (1992).

²⁰S. M. De Soto *et al.*, Phys. Rev. Lett. **70**, 2956 (1993).

²¹J. K. Clem, Phys. Rev. B **43**, 7837 (1991).

²²A. A. Gippius *et al.*, Physica C **276**, 57 (1997).

²³A. A. Gippius *et al.*, Phys. Rev. B **59**, 654 (1999).

²⁴S. D. Goren *et al.*, Physica C **313**, 127 (1999).

²⁵Y. Q. Song *et al.*, Phys. Rev. Lett. **70**, 3127 (1993).